Desalination and Water Treatment
www.deswater.com
doi: 10.1080/19443994.2013.868833

53 (2015) 2655–2663
March

Taylor & Francis
Taylor & Francis Group

Influence of Fe^{2+}-sodium persulfate on extracellular polymeric substances and dewaterability of sewage sludge

Yafei Shi[a], Jiakuan Yang[a,*], Wei Mao[a], Yalin Li[a], Xin Xu[a], Hao Zhang[a], Wenbo Yu[a], Ye Li[b], Changzhu Yang[a]

[a]*School of Environmental Science and Engineering, Huazhong University of Science and Technology, 1037# Luoyu Road, Wuhan, Hubei 430074, China*
Tel./Fax: +86 27 87792207; emails: jkyang@mail.hust.edu.cn; yjiakuan@hotmail.com
[b]*Universtar Science & Technology (Shenzhen) Co. Ltd., Shenzhen, Guangdong 518057, China*

Received 12 May 2013; Accepted 18 November 2013

ABSTRACT

Activated persulfate generated from Fe^{2+}-sodium persulfate (SPS) was used as a conditioner for dewatering of waste activated sludge. The effects of Fe^{2+}-SPS on dewaterability were investigated by specific resistance to filtration (SRF) and capillary suction time (CST), as well as further confirmed the results with diaphragm filter press dewatering process in laboratory. The amount of extracellular polymeric substances (EPS) and zeta potentials were analyzed. With 30 mg Fe^{2+} per gram dry solid (DS) and 100 mg SPS per gram DS, 89.0% of SRF and 84.1% of CST reductions were achieved, respectively. Furthermore, the dewatered cake moisture content was as low as 52.6% in the diaphragm filter press dewatering. The EPS fractions and zeta potential of the sludge floc were found to have significantly changed during the Fe^{2+}-SPS conditioning. Proteins and polysaccharides contents in filtrate all increased with increase in the amount of Fe^{2+}-SPS, but decreased in tightly bound EPS (TB-EPS). The change of proteins content in loosely bound EPS (LB-EPS) was more significant than polysaccharides. Scanning electron microscope images further demonstrated that the Fe^{2+}-SPS pre-treatment ruptured the sludge floc resulting in the formation of permeable and incompressibility structure in filtration process.

Keywords: Sewage sludge; Dewatering; Sulfate radical; Persulfate activation; Extracellular polymeric substances

1. Introduction

As activated sludge process is widely used in wastewater treatment, a large amount of waste activated sludge (WAS) being generated from such process needs to be treated or disposed of [1,2]. Due to composition and biological nature, WAS dewatering is one of the most challenging operations in sludge treatment [3,4]. Therefore, it requires conditioning prior to dewatering by chemical conditioners such as flocculants and coagulants [5–7]. Organic polymer has received more attention, and limitations are nearly invisible. First, centrifuge or belt press dewatering can

*Corresponding author.

only achieve a water content up to 80%, which fails to meet the requirements of incineration or landfill disposal [2]. Second, polymer residual bears long-term environmental risks that cannot be ignored when the dewatered sludge is disposed in landfill or compost. These shortcomings arouse urgent needs for alternative advanced sludge treatment methods by using environment-friendly conditioners to enhance dewaterability.

The activated persulfate oxidation, in recent years, receives attention as an alternative oxidant for soil and groundwater remediation [8,9]. It is a strong oxidizing agent (oxidation–reduction potential, E° = 2.01 V), which is non-selectively reactive and relatively stable at room temperature. If activated by heat, UV or a transition metal (M^{n+}) (Eq. (1)) [10], persulfate can initiate a free radical pathway through the formation of sulfate radicals (E° = 2.6 V), which can react with a wide range of environmental contaminants (Eq. (2)) [11–14]. The sulfate radicals can then propagate a serial free-radical reaction involving the formation of other active species (Eqs. (3) and (4)) [15].

$$S_2O_8^{2-} + 2M^{n+} \rightarrow 2M^{(n+1)+} + 2SO_4^{2-} \quad (1)$$

Through the following steps:

$$S_2O_8^{2-} + M^{n+} \rightarrow M^{(n+1)+} + SO_4^{-\bullet} + SO_4^{2-} \quad (1a)$$

$$SO_4^{-\bullet} + M^{n+} \rightarrow SO_4^{2-} + M^{(n+1)+} \quad (1b)$$

$$SO_4^{-\bullet} + RH \rightarrow R\bullet + HSO_4^- \quad (2)$$

$$SO_4^{-\bullet} + H_2O \rightarrow \bullet OH + SO_4^{2-} + H^+ \quad (3)$$

$$\bullet OH + RH \rightarrow R\bullet + H_2O \quad (4)$$

where RH represents an organic compound, and R· represents an oxidized organic compound. Sulfate radicals exhibit a higher standard reduction potential than hydroxyl radicals at neutral pH [16,17]. Although the classic Fenton's peroxidation is considered to be one of the effective pretreatments for sludge, it still has drawbacks and limitations. At a higher pH, such as pH > 6, aggregation and sedimentation of iron can greatly hamper its effectiveness. Therefore, pre-adjusting the acidity of sludge is inevitable and consequently increases operational cost and complexity of the process. In addition, some inorganic compounds in water will scavenge the free hydroxyl radicals [18]. On the contrary, sulfate radicals can overcome these limitations of the Fenton's peroxidation.

Although persulfate is capable of degrading a wide range of organic compounds, its use in sludge dewatering is still scarce [19,20], especially in diaphragm filter dewatering process. In this work, the effectiveness of Fe^{2+}-activated persulfate in improving sludge dewaterability was evaluated by the specific resistance to filtration (SRF) and the capillary suction time (CST). Furthermore, a laboratory scale experiment of sludge dewatering was carried out with Fe^{2+}-activated persulfate by diaphragm filter dewatering equipment. Finally, the influence of Fe^{2+}-activated persulfate on extracellular polymeric substances (EPS), including loosely bound EPS (LB-EPS) and tightly bound EPS (TB-EPS), zeta potentials were determined to explore the mechanism enhancing sludge dewaterability.

2. Materials and methods

2.1. Materials

The WAS samples were collected from the Longwangzui Wastewater Municipal Treatment Plant, Wuhan, which consisted of a homogeneous mixture of the primary and excess activated sludge. To minimize microbial activity, the samples were stored in a refrigerator (at 4℃ within 48 h). The sludge sample characteristics are shown in Table 1. Water content, total suspended solids (TSS), and volatile suspended solids (VSS) were measured following standard methods. SRF is 1.68×10^{13} m/kg and the CST is 225.9 s, representing typical WAS samples.

Sodium persulfate ($Na_2S_2O_8$, SPS) was obtained in solid (>99.5% purity) from Sinopharm Chemical Reagent Co. Ltd., Shanghai, China. Fe^{2+} solution was prepared from $FeSO_4{\cdot}7H_2O$ (>99.0% purity). All the chemical reagents are of analytical grade.

Table 1
Characteristics of the WAS sample

pH	Water content (wt.%)	COD (mg/L)	SCOD (mg/L)	VSS/TSS (%)	SRF ($\times 10^{13}$ m/kg)	CST (s)
6.88	96.55	20,200	1470.8	52.6	1.68	225.9

2.2. Sludge conditioning and dewaterability

A jar test apparatus was used for the sludge conditioning tests. A pre-determined amount of SPS was added to a 1 L beaker. The sludge samples were prepared by adding SPS in the 10–100 mg/g dry solid (DS) range and stirred at 300 rpm for 5 min. Thereafter, the Fe^{2+} solution (30–60 mg/g DS) was slowly injected into the mixed sample three times at 100 rpm for 20 min.

CST and SRF were used to evaluate the dewaterability in this study. The CST was measured using a 304M CST instrument (Triton, UK) equipped with a 10 mm diameter funnel. SRF was calculated using the following formula (Eq. (5)).

$$\mathrm{SRF} = \frac{2PA^2b}{\mu w} \tag{5}$$

where A is the area of the filter cake (m^2), P is the filtration pressure (N/m^2), b is the slope determined from the t/vol vs. vol plot; vol is the volume of filtrate, m^3; and t is the filtration time, s. μ is the viscosity of filtrate ($N{\cdot}s/m^2$), and w is the sludge solids concentration (kg/m^3).

2.3. Extraction of EPS and determination of EPS components

The contents of protein and polysaccharide in filtrate, LB-EPS and TB-EPS were measured to evaluate the Fe^{2+}-$S_2O_8^{2-}$ influence on the EPS-content of the samples. A modified heat extraction method [21,22] was used to extract the LB-EPS and TB-EPS from the WAS samples. A sludge suspension was first dewatered by centrifugation in a 50 mL tube at 4,000g for 5 min. The centrate liquor was recovered for water quality analysis. The sludge pellet in the tube was then resuspended into 15 mL of 0.05% NaCl solution. The sludge mixture was then diluted with the NaCl solution to its original volume of 50 mL. The NaCl solution for dilution was pre-heated to 70˚C to ensure that the sludge suspension reached an immediate warm temperature of 50˚C. Without any delay, the sludge suspension was then sheared for 1 min, followed by centrifugation at 4,000g for 10 min. The organic matter in the supernatant was readily extractable EPS and was regarded as the LB-EPS of the biomass. For the extraction of the TB-EPS, the sludge pellet left in the centrifuge tube was resuspended in 0.05% NaCl solution to its original volume of 50 mL. The sludge suspension was heated to 60˚C in a water bath for 30 min, and the sludge mixture was then centrifuged at 4,000g for 15 min. The supernatant that was collected was regarded as the TB-EPS extraction. The soluble fraction is the filtrate passing through the 0.45 μm filter membrane. The proteins were analyzed with the modified Lowry method [23] by using bovine serum albumin (Sigma). The polysaccharides content was tested with the anthrone method [24] by using glucose as the standard. Control tests were carried out concurrently without addition of any chemicals. All the experiments were carried out in duplicates.

2.4. Zeta potential

The zeta potentials of sludge are measured by a Brookhaven Zeta Plus (Brookhaven Instruments Corporation, USA), which measures the zeta potential of particles smaller than 3 μm. Therefore, in this work the zeta potential measured for sludge using this technique is similar to the reported by Thapa et al. [25]. The zeta potential of the sludge sample was obtained by centrifuging the sample for 10 min at 4,000 rpm. The zeta potentials reported here were calculated from the average of at least three measurements at 25˚C.

2.5. Diaphragm filter pressing test

A sketch of the sludge dewatering process in laboratory scale is shown in Fig. 1. The diaphragm filter press was equipped with six diaphragm plates (250 mm × 250 mm). Each side of the plate has a 10 mm depression. First, the sludge sample was conditioned with Fe^{2+}-SPS, and then pumped into a seal tank, in which the internal pressure was controlled by air pressure for feeding sludge to the filter press. Second, gradually increase the pressure to 0.8 MPa and until the effluent rate decreased. The filtrate was collected and weighed periodically during the process. Last, all diaphragm plates were injected with 1.2 MPa compressed air for about 20 min, which squeezed the diaphragm plates for further dewatering. After the

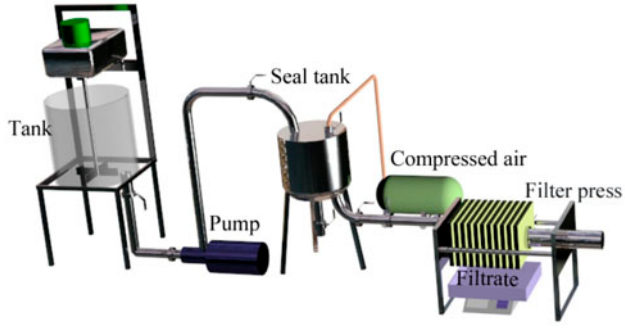

Fig. 1. The experimental set-up for diaphragm filter dewatering in laboratory scale.

pressure was released, the solid cakes inside each chamber were removed from the filter cloth and weighed. Its DS mass was determined by drying at 105℃ for 24 h and weighing.

2.6. Microstructural analysis

Scanning electron microscope (SEM) images were studied on sewage sludge dewatering samples before and after conditioning. Sludge samples were prepared by drying the samples at 45℃ and after coating with gold. The SEM (Sirion 200) was operated at 10 kV of acceleration voltage condition.

3. Results and discussion

3.1. Sludge dewaterability

The effects of SPS on SRF and CST at different Fe^{2+} dosages are depicted in Fig. 2. In all cases, higher SPS dosages caused larger reductions in SRF (Fig. 2(a)). When Fe^{2+} dosage is at 30 mg/g DS, the SRF of the conditioned sludge decreases to 1.179×10^{13} m/kg for 20 mg SPS/g DS (a 30.2% reduction) and to 0.189×10^{13} m/kg (an 89.0% reduction) for 100 mg SPS/g DS. Moreover, when the Fe^{2+} dosage is at 60 mg/g DS, SRF of the conditioned sludge decreases to 1.070×10^{13} and to 0.244×10^{13} m/kg with SPS dosages of 20 and 100 mg/g DS, respectively.

Results of CST tests are consistent with those of the SRF tests, as shown in Fig. 2(b). When Fe^{2+} dosage is at 30 mg/g DS, the CST of the conditioned sludge decreases to 135.4 (a 40.2% reduction) and to 35.9 s (an 84.1% reduction) by increasing SPS dosages from 10 to 100 mg/g DS. At Fe^{2+} dosage of 60 mg/g DS, CST shows a similar trend and decreases from 114.7 to 41.4 s with increasing SPS dosages from 10 to 100 mg/g DS. High dosage of SPS can improve the dewaterability of conditioned sludge reference to the SRF and CST reduction rate. When the SPS dosage is lower (less than 40 mg/g DS), the amount of $SO_4^{-}\cdot$ generated is not sufficient to react with the sludge particles to enhance the sludge dewaterability. As the SPS dosage increases, its concentration is high enough to produce $SO_4^{-}\cdot$. The results indicated that $SO_4^{-}\cdot$ plays an important role in the conditioning process. Furthermore, the dissolved Fe^{2+} is oxidized to Fe^{3+} (Eq. (1)), which will become insoluble and precipitates as ferric hydroxide in the Fe^{2+}-SPS system. These iron state changes could alter the physical character of flocs through co-precipitation of phosphorus, organics, and act as skeleton builder in sludge dewatering.

3.2. EPS contents

The proteins of raw sludge in filtrate, LB-EPS, and TB-EPS are 12.82, 12.52, and 130.70 mg/L; the polysaccharides are 4.67, 16.10, and 51.34 mg/L, respectively. Fig. 3 describes the effects of Fe^{2+}-SPS on EPS concentrations of the filtrate, LB-EPS, and TB-EPS when compared to that of the raw sludge. As shown in Fig. 3(a1), in all cases, the protein in the filtrate is higher than that of the raw sludge with various Fe^{2+} and SPS dosages. Especially, the corresponding protein contents significantly increase with the SPS dosage exceeding 40 mg/g DS. With the same SPS dosage, the protein content in the filtrate at 30 mg/g DS Fe^{2+} dosage is higher than that of 60 mg/g DS Fe^{2+} dosage. Generally, the protein in the filtrate increases with increasing SPS dosage at both different Fe^{2+} dosages. When the SPS dosage is at 100 mg/g DS, the protein content increases up to 77.97 mg/L. The change of the polysaccharide in the filtrate shows the same tendency as the protein in the filtrate, as shown in Fig. 3(b1). The polysaccharide concentration significantly increases (at SPS dosage less than 40 mg/g DS) for Fe^{2+} dosages of both 30 and 60 mg/g DS. The increase

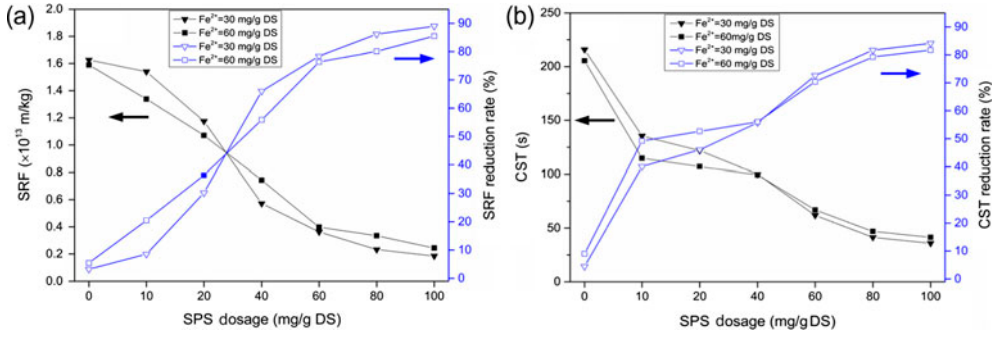

Fig. 2. Effects of Fe^{2+} and SPS dosages on (a) SRF and (b) CST of conditioned sludge.

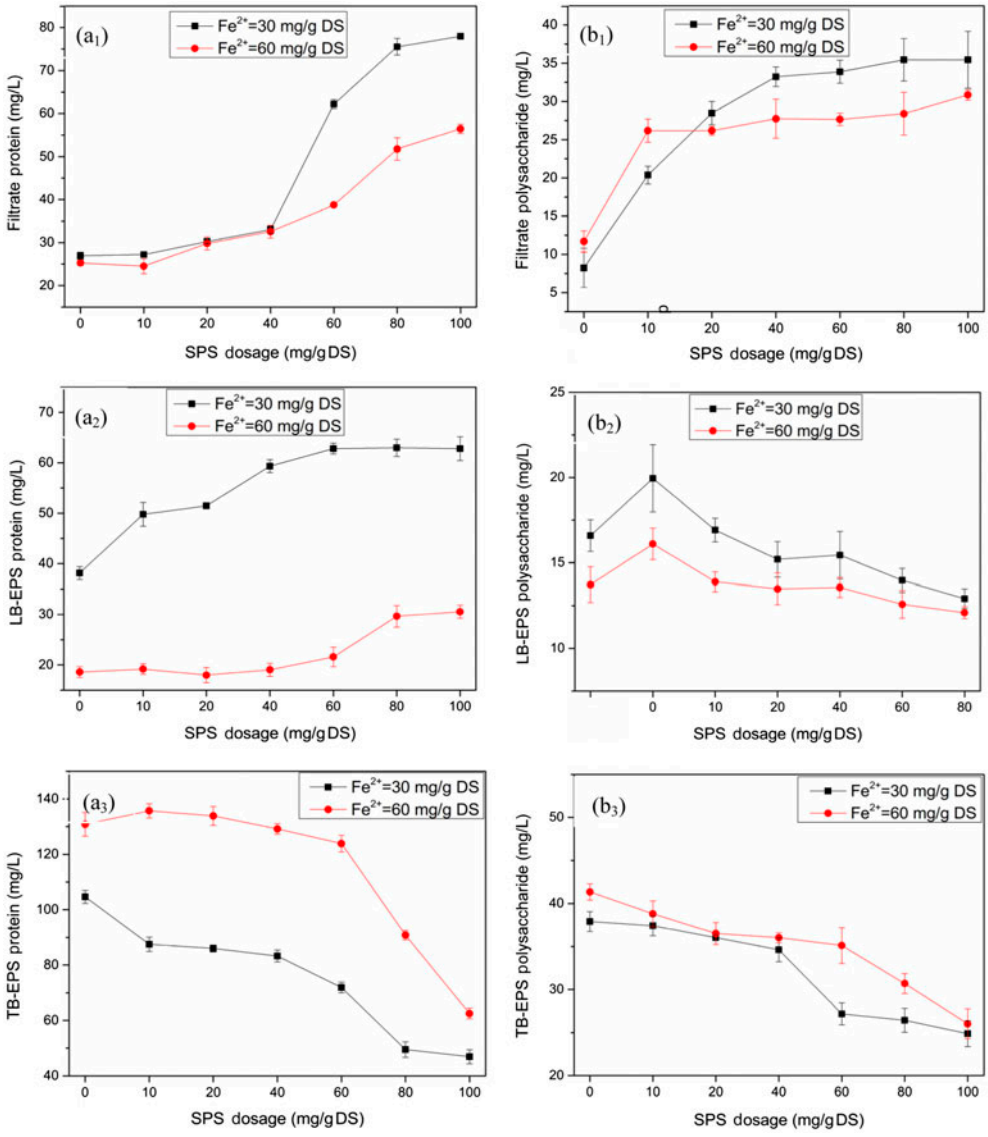

Fig. 3. The fate of proteins in filtrate (a1), LB-EPS (a2), and TB-EPS (a3), and polysaccharide in filtrate (b1), LB-EPS (b2), and TB-EPS (b3).

of protein and polysaccharide in the filtrate well explains that the flocs breakdown after conditioning by Fe^{2+} and SPS. The flocs enable to release some water trapped within the flocs to the bulk liquid phase, which tends to decrease the moisture content of the filter cake in diaphragm filter pressing test.

The experimental results show that the protein (Fig. 3(a2)) in the LB-EPS increases with increasing SPS dosage, whereas the polysaccharide (Fig. 3(b2)) in LB-EPS decreases with an increase of SPS dosage. When the SPS dosage is at 100 mg/g DS, the protein of the LB-EPS increases up to 62.81 and 30.55 mg/L with Fe^{2+} dosages of 30 and 60 mg/g DS, respectively. However, the polysaccharides decrease to 12.91 and 12.08 mg/L with the same dosages. The prediction can be made that $SO_4^{\cdot-}$ is likely to react with polysaccharide and protein in a different rate of degradation because of the different biochemical structure.

TB-EPS located in the inner flocs represents an essential structure and contributes to cell adhesion through strong interactions. TB-EPS fraction has a more strong water binding capability and more contribution to the sludge dewaterability than LB-EPS. Therefore, the collapse of TB-EPS was of a great

importance effect on the sludge dewaterability. Our results show that both of protein and polysaccharide content in the TB-EPS decrease with increasing SPS (Fig. 3(a3, b3)). The proteins in filtrate, LB-EPS or TB-EPS are significantly more than polysaccharides at the same Fe^{2+} and SPS dosages, which is consistent with that reported in literature [26].

When the SPS dosage is at 100 mg/g DS, proteins in the TB-EPS decrease to 46.91 and 62.52 mg/L with Fe^{2+} dosages of 30 and 60 mg/g DS, respectively. Likewise, the polysaccharide decreases to 24.87 and 26.02 mg/L with the same dosages. This can be attributed partially to the fact that $SO_4^{\cdot-}$ breaks up the sludge matrix and makes more oxidation of TB-EPS. Thus, $SO_4^{\cdot-}$ generated from Fe^{2+}-SPS could enhance the sludge dewaterability, which is consistent with the CST and SRF results in Section 3.2.

3.3. Zeta potential changes

The effect of Fe^{2+}-SPS on the surface charge of sludge was investigated by measuring the zeta potential of the centrate obtained from centrifuging the sludge flocculated at different Fe^{2+} and SPS doses. The results of the zeta potential measurements are shown in Fig. 4. The surfaces of the WAS are originally negatively charged with the zeta potential of −14.1 mV. When the SPS dosage is at 100 mg/g DS, the zeta potential of the sludge increases to 9.2 and 5.0 mV with Fe^{2+} dosages of 30 and 60 mg/g DS, respectively. It is known that increasing the SPS dosages results in an increase in zeta potential and charge reversal of the particle.

Zeta potentials stabilize at approximately 3.0 mV by the two Fe^{2+} dosages with a dosage range from 10 to 40 mg SPS/g DS, respectively. However, a further increase in SPS dosage results in a slight increase in the zeta potential. As for the sludge conditioned with the SPS from 60 to 100 mg/g DS, followed by 30 mg Fe^{2+}/g DS, the zeta potential ranges from 5.6 to 9.2 mV. However, followed by 60 mg Fe^{2+}/g DS, the zeta potential is at an approximately constant value of 4.5 mV.

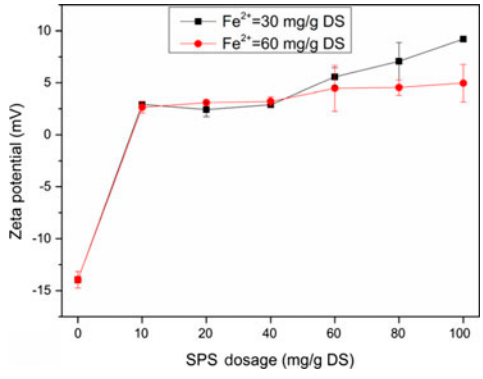

Fig. 4. Variations of zeta potential at different SPS and Fe^{2+} dosages.

When the sludge was conditioned with Fe^{2+}-SPS, the zeta potential became strongly positive, indicating that positive colloids generated in the Fe^{2+}-SPS system. It is found that the optimum dosage of Fe^{2+}-SPS, on the basis of SRF and CST results, not occurs at the point of zero charge, while the excellent dewaterability of sludge can be achieved when sludge particles carry a positive charge (i.e. 4.96 mV). This suggests that electrostatic forces might not predominantly control the enhanced dewatering from Fe^{2+}-SPS conditioning [5].

EPS fractions of the sludge flocs are related to the zeta potential. Liao et al. [27] have reported that the moderate correlation between the proportions of EPS components and the surface charge indicates that other factors and/or EPS components may be contributing to the surface charge properties of microbial floc. As it has been presented in Section 3.2, the proteins in filtrate increased with the increase of Fe^{2+}-SPS dosages. Therefore, the more the proteins are released from sludge flocs to liquid phase, the more the contribution the increasing of EPS charges in the presence of Fe^{2+}-SPS, as well as zeta potential. This finding is in accordance with the report by Mikkelsen et al. [28], they noted that increasing EPS fractions as well as increased zeta potential, especially proteins and humics were the main contributors to EPS charges, whereas the polysaccharide was lower on a mass basis and correlated poorly to the EPS charge content. Furthermore, ferric and ferrous irons increase charge density that could strengthen the impact under Fe^{2+}-SPS conditioning.

3.4. Diaphragm filter press dewatering

Based on the results of above-mentioned measurements of SRF and CST, 30 mg Fe^{2+}/g DS and 100 mg SPS/g DS were used in the diaphragm filter press dewatering experiment.

The filtrate-feed during the dewatering process and pictures of the dewatered filter cakes are shown in Fig. 5. All the diaphragm filter dewatering experiments were carried out with the same feed pressure procedure, shown in Fig. 5(a). First, the "step up" input pressure of the variation in the filtration pressure over a period of time until to 0.8 MPa, which

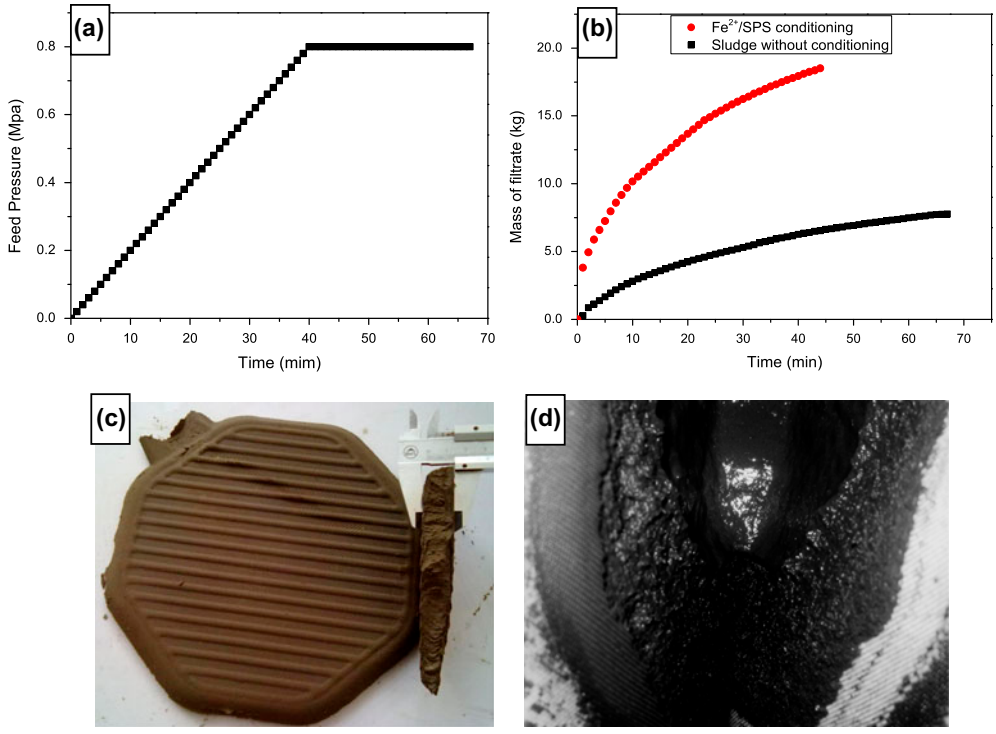

Fig. 5. The results of diaphragm filter pressing test: (a) the plot of feed pressure versus time, (b) the plot of filtrate mass versus time, (c) pictures of the dewatered sludge cake with Fe^{2+}/SPS conditioning, and (d) dewatered sludge cake without any conditioner.

improved the efficiency of sludge expression, has been described by Raynaud et al. [29]. Then, the constant pressure phase occurs at a later stage of the process. Both the total filtrate mass and the filtration rate with Fe^{2+}-SPS conditioning are significantly higher than those without conditioning (Fig. 5(b)). It implies that the sludge dewaterability is significantly improved with Fe^{2+}-SPS conditioning.

The dewatered cake moisture content is as low as 52.6%, and retains a solid shape, as shown in Fig. 5(c), while the raw sludge without any conditioner is unable to form a filter cake (Fig. 5(d)) even after a long dewatering time (1.5 times of that with Fe^{2+}-SPS conditioning). The result is consistent with the jar test; Fe^{2+}-SPS conditioning improves the sludge dewatering performance.

3.5. Microscopic structure

The microscopic structure of the freeze-dried samples was visualized to confirm the porosity of the sludge cake, as shown in Fig. 6. Fig. 6 (a) and (b)

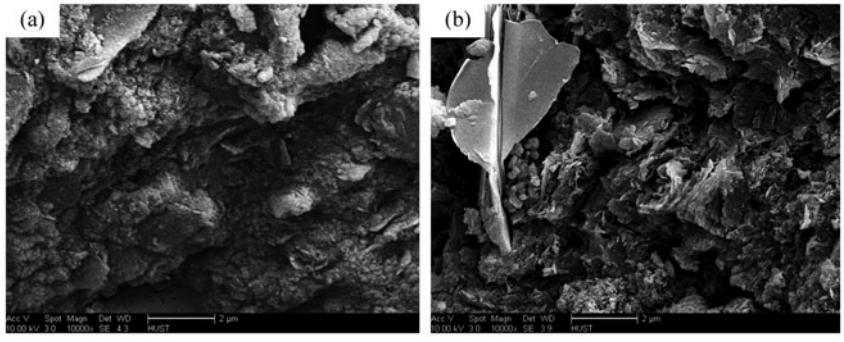

Fig. 6. SEM images of raw sludge (a) and sludge cake with Fe^{2+}/SPS conditioning (b).

show SEM images of the sludge filter cake samples without any conditioning and with Fe^{2+}-SPS conditioning comparatively. The morphology of the raw sludge presents dense and smooth surface (Fig. 6(a)). This dense structure, thought to be colloidal in flocs, could lead to the formation of a "filter skin" made up of highly compressible colloids that would create the major resistance to filtration of sludge cakes, which may be mainly resulting in impermeable and compressible structure in filtration process. As shown in Fig. 6(b), the conditioned sample shows a porous and coarse structure. The results indicate that Fe^{2+}-SPS conditioning resulted in the degradation of protein and polysaccharide in the flocs and affected the sludge structure. The formation of the filter cakes are open, porous structures of high permeability during dewatering by mechanical filtering.

4. Conclusions

Both SRF and CST of samples significantly decreased after Fe^{2+}-SPS conditioning. An 89.0% reduction in SRF and an 84.1% reduction in CST were obtained with Fe^{2+}-SPS conditioning, when compared to those without conditioning. The EPS fractions, zeta potential of the sludge floc were found to have significantly changed during the Fe^{2+}-SPS conditioning. The data decreased that the proteins and polysaccharides contents in filtrate all increase with increasing the amount of Fe^{2+}-SPS, whereas decrease in TB-EPS under higher dosage of Fe^{2+}-SPS. The change of proteins content in LB-EPS appeared to be more obvious than polysaccharides. SEM images further demonstrate that the Fe^{2+}-SPS pre-treatment ruptured the sludge floc. The conditioned sludge presented many laxity pores and coarse morphology, and the water in the intracellular space was released into the solution, which could enhance the dewaterability of sludge in the diaphragm filter press dewatering process.

Acknowledgments

The author would like to appreciate the financial support provided by the National Natural Science Foundation of China (51078162), the Wuhan Planning Project of Science and Technology (201260723226), the Fundamental Research Funds for the Central Universities (2013TS071), the Research Project of Chinese Ministry of Education (113046A), and the Project on Technical of Research and Development of Shenzhen (CXY201106210008A). The authors would also like to thank the Analytical and Testing Center of Huazhong University of Science and Technology, for providing the facilities for the experimental measurements.

References

[1] H. Saveyn, D. Curvers, O. Thas, P. Van der Meeren, Optimization of sewage sludge conditioning and pressure dewatering by statistical modelling, Water Res. 42 (2008) 1061–1074.
[2] H. Liu, J.K. Yang, Y.F. Shi, Y. Li, S. He, C.Z. Yang, H. Yao, Conditioning of sewage sludge by Fenton's reagent combined with skeleton builders, Chemosphere 88 (2012) 235–239.
[3] M.L. Christensen, K. Keiding, Creep effects in activated sludge filter cakes, Powder Technol. 177 (2007) 23–33.
[4] D. Curvers, S.P. Usher, A.R. Kilcullen, P.J. Scales, H. Saveyn, P. Van der Meeren, The influence of ionic strength and osmotic pressure on the dewatering behaviour of sewage sludge, Chem. Eng. Sci. 64 (2009) 2448–2454.
[5] C.H. Lee, J.C. Liu, Sludge dewaterability and floc structure in dual polymer conditioning, Adv. Environ. Res. 5 (2001) 129–136.
[6] B. Bolto, J. Gregory, Organic polyelectrolytes in water treatment, Water Res. 41 (2007) 2301–2324.
[7] S.K. Dentel, Chemical conditioning for solid-liquid separation processes, Dry. Technol. 28 (2010) 843–849.
[8] C. Cuypers, T. Grotenhuis, K.G. Nierop, E.M. Franco, A. de Jager, W. Rulkens, Amorphous and condensed organic matter domains: The effect of persulfate oxidation on the composition of soil/sediment organic matter, Chemosphere 48 (2002) 919–931.
[9] M. Ahmad, A.L. Teel, R.J. Watts, Persulfate activation by subsurface minerals, J. Contam. Hydrol. 115 (2010) 34–45.
[10] C. Liang, C.J. Bruell, M.C. Marley, K.L. Sperry, Persulfate oxidation for *in situ* remediation of TCE. I. Activated by ferrous ion with and without a persulfate–thiosulfate redox couple, Chemosphere 55 (2004) 1213–1223.
[11] S.Y. Oh, H.W. Kim, J.M. Park, H.S. Park, C. Yoon, Oxidation of polyvinyl alcohol by persulfate activated with heat, Fe^{2+}, and zero-valent iron, J. Hazard. Mater. 168 (2009) 346–351.
[12] O.S. Furman, A.L. Teel, R.J. Watts, Mechanism of base activation of persulfate, Environ. Sci. Technol. 44 (2010) 6423–6428.
[13] S.D. Richardson, B.L. Lebron, C.T. Miller, M.D. Aitken, Recovery of phenanthrene-degrading bacteria after simulated *in situ* persulfate oxidation in contaminated soil, Environ. Sci. Technol. 45 (2011) 719–725.
[14] A. Tsitonaki, B. Petri, M. Crimi, H. Mosbaek, R.L. Siegrist, P.L. Bjerg, In situ chemical oxidation of contaminated soil and groundwater using persulfate: A review, Crit. Rev. Env. Sci. Technol. 40 (2010) 55–91.
[15] J. Costanza, G. Otaño, J. Callaghan, K.D. Pennell, PCE oxidation by sodium persulfate in the presence of solids, Environ. Sci. Technol. 44 (2010) 9445–9450.
[16] G.P. Anipsitakis, D.D. Dionysiou, Radical generation by the interaction of transition metals with common oxidants, Environ. Sci. Technol. 38 (2004) 3705–3712.

[17] C. Liang, Z.S. Wang, C.J. Bruell, Influence of pH on persulfate oxidation of TCE at ambient temperatures, Chemosphere 66 (2007) 106–113.
[18] J. Kochany, E. Lipczynska-Kochany, Application of the EPR spin-trapping technique for the investigation of the reactions of carbonate, bicarbonate, and phosphate anions with hydroxyl radicals generated by the photolysis of H_2O_2, Chemosphere 25 (1992) 1769–1782.
[19] G. Zhen, X. Lu, Y. Zhao, X. Chai, D. Niu, Enhanced dewaterability of sewage sludge in the presence of Fe (II)-activated persulfate oxidation, Bioresour. Technol. 116 (2012) 259–265.
[20] G.Y. Zhen, X.Q. Lu, Y.Y. Li, Y.C. Zhao, B.Y. Wang, Y. Song, X.L. Chai, D.J. Niu, X.Y. Cao, Novel insights into enhanced dewaterability of waste activated sludge by Fe(II)-activated persulfate oxidation, Bioresour. Technol. 119 (2012) 7–14.
[21] J.W. Morgan, C.F. Forster, L. Evison, A comparative study of the nature of biopolymers extracted from anaerobic and activated sludges, Water Res. 24 (1990) 743–750.
[22] X.Y. Li, S.F. Yang, Influence of loosely bound extracellular polymeric substances (EPS) on the flocculation, sedimentation and dewaterability of activated sludge, Water Res. 41 (2007) 1022–1030.
[23] B. Frølund, R. Palmgren, K. Keiding, P.H. Nielsen, Extraction of extracellular polymers from activated sludge using a cation exchange resin, Water Res. 30 (1996) 1749–1758.
[24] A.F. Gaudy, Colorimetric determination of protein and carbohydrate, Lndust. Water Wastes 7 (1962) 17–22.
[25] K.B. Thapa, Y. Qi, A.F.A. Hoadley, Interaction of polyelectrolyte with digested sewage sludge and lignite in sludge dewatering, Colloids Surf., A 334 (2009) 66–73.
[26] C. Park, J.T. Novak, R.F. Helm, Y.O. Ahn, A. Esen, Evaluation of the extracellular proteins in full-scale activated sludges, Water Res. 42 (2008) 3879–3889.
[27] B.Q. Liao, D.G. Allen, I.G. Droppo, G.G. Leppard, S.N. Liss, Surface properties of sludge and their role in bioflocculation and settleability, Water Res. 35 (2001) 339–350.
[28] L.H. Mikkelsen, K. Keiding, Physico-chemical characteristics of full scale sewage sludges with implications to dewatering, Water Res. 36 (2002) 2451–2462.
[29] M. Raynaud, P. Heritier, J.C. Baudez, J. Vaxelaire, Experimental characterisation of activated sludge behaviour during mechanical expression, Process Saf. Environ. 88 (2010) 200–206.